Exact three-dimensional spectral solution to surface-groundwater interactions with arbitrary surface topography

Anders Wörman,[1] Aaron I. Packman,[2] Lars Marklund,[1] Judson W. Harvey,[3] and Susa H. Stone[2]

Received 19 January 2006; revised 22 February 2006; accepted 1 March 2006; published 7 April 2006.

[1] It has been long known that land surface topography governs both groundwater flow patterns at the regional-to-continental scale and on smaller scales such as in the hyporheic zone of streams. Here we show that the surface topography can be separated in a Fourier-series spectrum that provides an exact solution of the underlying three-dimensional groundwater flows. The new spectral solution offers a practical tool for fast calculation of subsurface flows in different hydrological applications and provides a theoretical platform for advancing conceptual understanding of the effect of landscape topography on subsurface flows. We also show how the spectrum of surface topography influences the residence time distribution for subsurface flows. The study indicates that the subsurface head variation decays exponentially with depth faster than it would with equivalent two-dimensional features, resulting in a shallower flow interaction. **Citation:** Wörman, A., A. I. Packman, L. Marklund, J. W. Harvey, and S. H. Stone (2006), Exact three-dimensional spectral solution to surface-groundwater interactions with arbitrary surface topography, *Geophys. Res. Lett.*, *33*, L07402, doi:10.1029/2006GL025747.

1. Introduction

[2] Surface-groundwater flow interactions play an important role in water resources and aquatic ecosystems [*Thibodeaux and Boyle*, 1987; *Alley et al.*, 2002], mediate nutrient dynamics and contaminant transport [*Allan*, 1995], and must be considered in the design of long-term nuclear waste repositories [*Tóth and Sheng*, 1996; *Gascoyne*, 2003]. The interaction between surface water and groundwater flows is controlled by surface topography because pressure variations are induced by stream flow over sediment bedforms [*Thibodeaux and Boyle*, 1987; *Shen et al.*, 1990; *Harvey and Bencala*, 1993; *Elliott and Brooks*, 1997] and, at the landscape scale, the groundwater surface generally follows the ground surface [*O'Loughlin*, 1986].

[3] Based on such a premise, several researchers have derived exact solutions of the subsurface flow field [*Bervoets et al.*, 1991; *Elliott and Brooks*, 1997; *Packman and Bencala*, 2000]. *Tóth* [1962] and *Zijl* [1999] used superposition principles to represent solutions for a spectrum of topographical scales. To date, however, it has not been possible to determine induced surface-groundwater flows exactly in three dimensions for arbitrary topography. One reason has been that the harmonic function investigated by *Bervoets et al.* [1991] and *Zijl* [1999] describes topography that is uniform in the direction of the vector $[k_x, k_y]$, where k_x and k_y are wavenumbers in the x- and y-directions (Figures S1 and S2).[1] This uniformity is similar to the two-dimensional formulation adopted by *Elliott and Brooks* [1997].

[4] Here we develop a new three-dimensional spectral solution with harmonic functions that are independent in the x- and y-directions and demonstrate its applicability in various 3D hydrological applications using data over a wide range of spatial scales.

2. Theoretical Advancements

2.1. Spectral Solution and Boundary Condition Spectra

[5] The superposition principle can be applied to potential (Darcy) groundwater flow if the flow domain has a flat upper surface (i.e., the geometry is the same for all superimposed solutions). This simplification has been found acceptable for analyses of both hyporheic exchange [*Elliott and Brooks*, 1997; *Packman and Bencala*, 2000] and large-scale groundwater flow [*Zijl*, 1999]. If the Fourier series terms include an appropriate decay function with depth, they are exact solutions to the groundwater flow in either two or three dimensions. Further, they are orthogonal functions and, as such, are convenient tools to interpret the spectrum of landscape topography.

[6] Homogeneous, stationary and laminar (Darcy) groundwater flow follows Laplace equation, $\nabla^2 h = 0$, where ∇ = Nabla operator and h = energy potential of the groundwater flow (hydraulic head) [m]. To provide a suitable representation of the subsurface flow, we assume no-flow condition at the depth ε, i.e., $\partial c/\partial z|_{z=\varepsilon} = 0$, and a flat upper boundary with a given head variation at depth z = 0; i.e., h(x, y, z = 0), where (x, y, z) are Cartesian coordinates (z positive upward) and ε = depth to impermeable surface [m].

[7] The following Fourier series satisfy Laplace equation for the above conditions (Figure S3) and, because it is non-uniform in the (x, y) plane, is well-suited for topographical fitting:

$$h(x,y,z) = \langle h \rangle + \sum_{j=1}^{N_y}\sum_{i=1}^{N_x} (h_m)_{i,j} \cdot \frac{\exp\left(\sqrt{k_{x,i}^2 + k_{y,j}^2}z\right) + \exp\left(\sqrt{k_{x,i}^2 + k_{y,j}^2}(-2\varepsilon - z)\right)}{1 + \exp\left(-2\sqrt{k_{x,i}^2 + k_{y,j}^2}\varepsilon\right)} \cdot \sin\left(k_{x,i}x\right)\cos\left(k_{y,j}y\right) \quad (1)$$

[1]Department of Biometry and Engineering, Swedish University of Agricultural Sciences, Uppsala, Sweden.
[2]Department of Department of Civil and Environmental Engineering, Northwestern University, Evanston, Illinois, USA.
[3]U.S. Geological Survey, Reston, Virginia, USA.

0094-8276/06/2006GL025747$05.00

[1]Auxiliary material is available at ftp://ftp.agu.org/apend/gl/2006gl025747.

in which $0 \le z \le \varepsilon$, $(h_m)_{i,j}$ = amplitude coefficients [m], $\langle \ldots \rangle$ = aerial arithmetic mean value, N = number of wavelengths in the x- and y-directions, $k = 2\pi/\lambda$ is the wave number and λ [m] is wave length and. Each Fourier term of (1) represents a partial solution to the groundwater flow field related to a specific wave number of the energy potential at the groundwater surface.

[8] While the use of the Fourier solution does not depend on the exact type of head boundary condition, two generally accepted relationships are utilized here. Firstly, at the landscape scale, the groundwater surface and its energy potential generally follows land topography; i.e., H(x, y) = Z(x, y), where H is the phreatic surface h(x, y, z = 0) and Z is the ground surface elevation; i.e., h(x, y, z = 0) = Z(x, y). Secondly, in stream flows the gradient in H(x, y) drives the mean flow and there is an additional component due to the dynamic head arising at the stream bottom due to the stream flow deflection against an uneven bed-surface [*Shen et al.*, 1990; *Harvey and Bencala*, 1993]. Here the dynamic head follows the bed topography with a phase shift, ζ (m), and amplitude due to the stream velocity, V (m/s), following the approach of *Elliott and Brooks* [1997]:

$$h(x,y,z=0) = H(x,y) + 0.28\frac{V^2}{2g}\left(\frac{\sigma_h/d}{0.34}\right)^{3/8}(\langle Z\rangle - Z(x+\zeta,y))$$
$$= \langle h\rangle + \sum_{j=1}^{N_y}\sum_{i=1}^{N_x}(h_m)_{i,j}\sin(k_{x,i}x)\sin(k_{y,j}y) \qquad (2)$$

where d is the mean stream depth, σ_h is the standard deviation of h, and g is the acceleration due to gravity.

[9] The subsurface velocity field is readily obtained from the head distribution, (1), as $\mathbf{q} = K\nabla h$, where $\mathbf{q}$ is the Darcy velocity vector, K is the hydraulic conductivity and ∇ is the Nabla operator. Streamlines and residence time distributions are obtained easily from the flow field using a numerical particle tracking routine.

2.2. Numerical Evaluation of Fourier Coefficients From Topographical Data

[10] The topographical fitting requires that the amplitude coefficients be evaluated for a pre-assigned spectrum (series) of $k_x = 2\pi/\lambda_x$ and $k_y = 2\pi/\lambda_y$, where λ is wavelength. Hence, equation (1) can represent several topography observations in the form of $\mathbf{CH} = \mathbf{Z}$, in which $\mathbf{C}$ is a $Mx(N_xN_y)$ coefficient matrix containing the pre-assigned harmonics of (1), $\mathbf{H}$ contains the $(N_xN_y)x1$ amplitudes h_m and $\mathbf{Z}$ a Mx1 vector containing the observed h-values in M locations. A least-square estimation of the amplitude vector is obtained as $\mathbf{H} = [\mathbf{C}^T\mathbf{C}]^{-1}\mathbf{C}^T\mathbf{Z}$.

[11] Restrictions must be imposed on evaluation of the Fourier coefficients. Because it is often necessary to include a large number of terms, the function can adopt undesired shapes outside the fitting area that can affect the flow field inside the domain of interest. To avoid this, the coefficients are restricted by sparse data points significantly outside the area of interest. Hence, the domain is extended by mirroring at least four times, producing a 16 times larger area with periodic topography (Figure S4 and computer codes in auxiliary material). The artificial symmetry conditions counteract the effect of undesired function shapes and provide a smooth surface in the primary domain. This ensures low bias in the groundwater flow field.

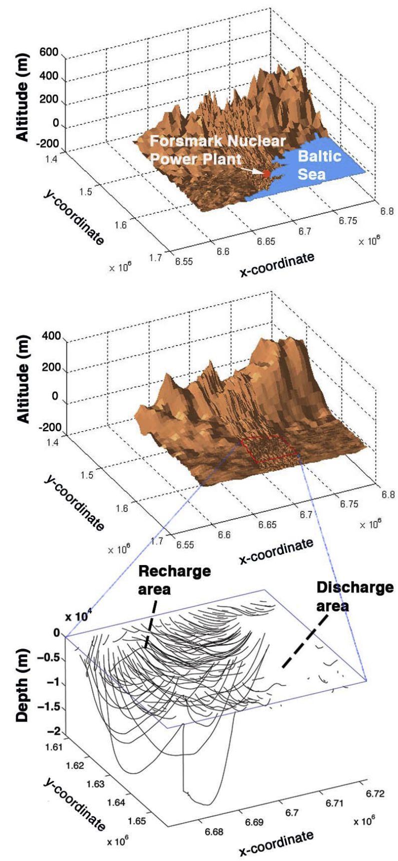

Figure 1. (top) Map data from the Swedish National Land Survey covering an area of 40,000 km^2 (middle) with the National coordinate system RT 90 compared with Fourier surface using 784 terms. Higher resolution around the central area marked with a red rectangle gives higher weight of this area when the Fourier coefficients are determined. (bottom) Flow trajectories with dis- and recharge areas with assumption of groundwater flow extending to a depth of 20 km in the crust.

[12] Flow domains with aspect ratios far from unity in the horizontal plane may require an anisotropic distribution of wavelengths. An appropriate value of the longest wavelength is one to two times the domain length in each direction. In addition, the shortest wavelength should not fall below the resolution of the data used to define the surface topography.

3. Accuracy of Analysis of Groundwater Flow

[13] The spectral method can readily be applied to analyze large-scale groundwater flows. Figure 1 shows elevation data of a 40,000 km^2 landscape in Northern Uppland, Sweden, the Fourier-series representation based on equation (1) using 784 terms, and the resulting subsurface flow patterns. The error of the fit relative to the total altitude difference in the domain is about 1.8%. The topographical spectrum for this landscape, similar to that shown in Figure 2, indicates that the vast majority of the landscape features are characterised by small values of h_m/λ_x, where h_m is amplitude of hydraulic head. These shallow features do not have a substantial influence on

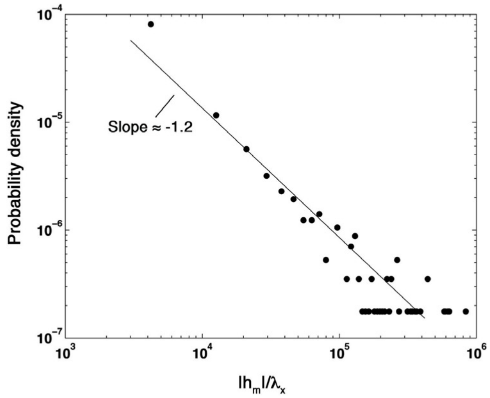

Figure 2. Spectrum of hydraulic head in Sugar Creek using 784 terms in the Fourier series. The frequency decays with increasing amplitude-to-wavelength ratio, $|h_m|/\lambda_x$. Essentially, the data set does not contain enough points to provide a statistically high-quality representation of the infrequent features contained in the tail of the topographic distribution.

hydraulic gradients in the subsurface. Features with high impact on surface-groundwater interaction, with large steepness h_m/λ_x, occur with low frequency.

[14] Numerical analyses indicate that the assumption of a flat upper surface in the solution domain produces an error of less than 20% in the water flux across the upper boundary of a single harmonic when $h_m/\lambda < 0.2$ and $0.1 < \varepsilon/\lambda$ (Figure S5). The error associated with complicated topography, like shown in Figure 1, can be approximated from the best single harmonic representing the surface (not from the sum of each harmonic in a series). Numerical perturbations that appear in the Fourier function can also be avoided by representing the flow only at depths deeper than the smallest wavelength used to represent the surface topography.

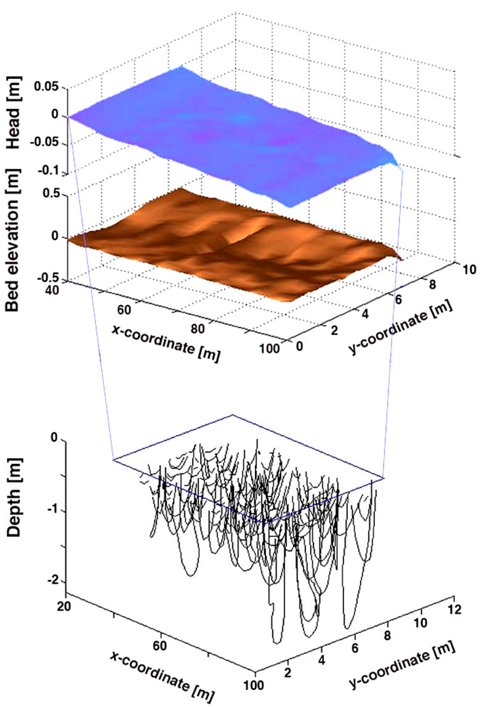

Figure 3. (top) Fourier representation of the topography of 6 m × 50 m reach of Sugar Creek constructed from 498 measured elevations (copper toned surface) and hydraulic head according to equation (2) (blue surface, offset vertically by 0.3 m for clarity). The topography fit has a relative error of less than 1%. (bottom) The calculated hyporheic flow paths. The Fourier interpretations include 676 terms with anisotropic wavelengths.

4. Analysis of Hyporheic Exchange in Streams

[15] The spectral method is applied also to the stream-subsurface flow interaction and its effect on solute transport in a 50 m-long reach of Sugar Creek, a headwater tributary of the Mississippi River in north-western Indiana, USA. An in-stream tracer injection was performed with KBr following the procedures of *Harvey and Bencala* [1990], and the resulting solute breakthrough curve is analysed following *Wörman et al.* [2002]. Water and bed surface elevations were measured using a wading rod and velocity profiles were measured using a Sontek Flowtracker ADV in cross-sections at a downstream interval of 5 m. The local streambed topography was measured at five of these locations using a submersible laser distance meter.

[16] Figure 3 shows the channel bathymetry, boundary head surface, and subsurface flow trajectories using the Fourier method and Figure 2 shows the spectra of hydraulic head over the bed surface. Figure 4 compares the predicted hyporheic residence time distribution with the one obtained from analysis of the solute tracer data (Figure S6). The spectral method represents the channel topography with a relative error of less than 1%. Both data and Fourier analysis indicated that there is a bimodal distribution of solute retention times in the study reach. Similar multiple time-scales of hyporheic exchange were previously noted by *Choi et al.* [2000], *Haggerty et al.* [2002] and *Wörman et al.* [2002].

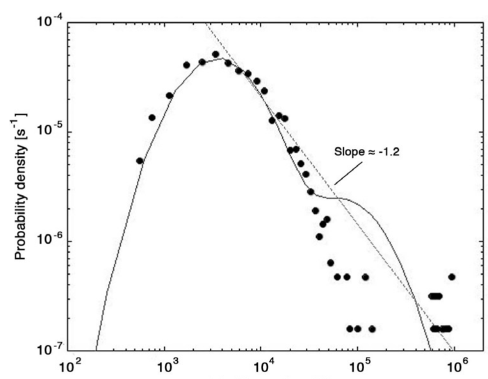

Figure 4. Residence time probability density function (PDF) for hyporheic exchange in Sugar Creek evaluated from tracer experiment results (solid curve) and particle tracking analysis based on 2,600 particles and the calculated flow field shown in Figure 3 (dots). The solid curve is a bimodal log-normal distribution included in the ASP model [*Wörman et al.*, 2002] and which is calibrated versus the tracer data. Both model interpretation of tracer data (solid curve) and simulated residence time PDF (dots) indicate a bimodal distribution of subsurface residence times reflecting two distinct scales of bed surface topography.

[17] The bimodal character of the residence time probability density function (PDF) can be explained by a bimodal size distribution of the streambed topography. This study provides a theoretical platform for linking the multiple time-scales of hyporheic solute transport with the controlling scales of channel morphology. Figure 4 shows good agreement between the residence time PDF obtained from the tracer data and the corresponding distribution obtained from the spectral analysis. The spectral analysis reveals that the two peaks of the bimodal distribution reflect the relatively rapid hyporheic exchange induced by bed roughness elements with wavelengths on the order of 0.5 m and 10 m.

5. Implications

[18] The spectral representation, equation (1), is an exact solution for the surface-subsurface water interaction and can be applied to various hydrological applications over a wide range of geometrical scales. Subsurface flow develops a distribution of circulation cells, which makes it difficult to analyze isolated "local" subsurface flow domains. Figures 1 and 3 clearly show that topographic divides do not limit subsurface flows, because all topographical features affect the flow at any location. The spectral method independently resolves the effect on the flow of each topographical scale in the spectrum. This method opens new possibilities for analysis of surface-groundwater interactions, such as studies of the effects of land surface topography on groundwater flows from the local aquifer scale to the scale of entire continents.

[19] Groundwater flow in a system with many superimposed topographical features typically becomes stagnant in some specific regions at various depths. The spectral method reveals that this phenomenon is directly related to the superposition of flows induced at several geometrical frequencies that counteract each other. Such stagnant zones are found in the examples presented here. At large scales, such as that analyzed in Figure 1, water can be retained in these stagnant zones for very long periods of time – millions of years.

[20] Both the slopes of the h_m/λ_x spectrum and the power-law tail of subsurface residence time distribution found in Sugar Creek both have values between −1.1 and −1.2. While it is known that the retention times of water and dissolved constituents in stream systems are highly skewed in their distribution with a slope between −0.7 and −1.2 [*Kirchner et al.*, 2000; *Haggerty et al.*, 2002], this analyses suggest that the three-dimensional nature of the problem imposes a more complicated residence time behaviour when the full range of topographical scales are considered. The PDFs for residence time and h_m/λ are related due to the linear relationships h_m/λ vs. the gradient of hydraulic head, hydraulic gradient vs. water flow velocity and water flow velocity and residence times.

[21] The three-dimensional spectral analysis shows a fundamental difference from two-dimensional interfacial flows. From equation (1), the subsurface head variation decays with depth as $e^{\sqrt{2}kz}$ when $k_x = k_y$ (z is negative). This is a faster decay with depth than found in two-dimensional flow solutions, which have been shown to decay as e^{kz}[*Elliott and Brooks*, 1997; *Zijl*, 1999]. Consequently, the 3D flow has a shallower flow interaction and slightly shorter mean subsurface residence time than the 2D flow. The tail of the 3D distribution dies off more rapidly. While the effects of small-scale topographic features attenuate with depth faster than suggested by prior analyses, all topographic scales contribute to the total water flux across the ground surface.

[22] Beyond clarifying the effects of 3D flows, the method presented here also enables straightforward prediction of induced subsurface flows. While the method is currently limited to homogeneous hydraulic conductivity, it is rapid and useful for preliminary site evaluations.

[23] **Acknowledgments.** This study was financially supported by the Swedish Nuclear Power Inspectorate, the Swedish Radiation Protection Authority and the U.S. National Science Foundation under grant number EAR-0408744. We thank Lisa Marx and Joel Detty for help with the Sugar Creek test, and Kenneth E. Bencala, Luis Amaral and anonymous reviewers for comments on the paper.

References

Allan, J. D. (1995), *Stream Ecology: Structure and Function of Running Waters*, Chapman and Hall, London.

Alley, W. A., R. W. Healy, J. W. LaBaugh, and T. E. Reilly (2002), Flow and storage in groundwater systems, *Science*, *296*, 1985–1990, doi:10.1126/science.1067123.

Bervoets, A. F., W. Zijl, and M. van Veldhuizen (1991), Spatial scale analysis of groundwater flow pattern for transport in sedimentary basins, in Modelling and Control of Water Resource Systems and Global Changes, edited by E. J. H. Kerckhoffs et al., Soc. for Comput. Simul. Int., 167–172, Ghent, Belgium.

Choi, J., J. W. Harvey, and M. H. Conklin (2000), Characterizing multiple timescales of stream and storage zone interaction that affect solute fate and transport in streams, *Water Resour. Res.*, *36*, 1511–1518.

Elliott, A. H., and N. H. Brooks (1997), Transfer of nonsorbing solutes to a streambed with bed forms: Theory, *Water Resour. Res.*, *33*, 123–136.

Gascoyne, M. (2003), Hydrogeochemistry, groundwater ages and sources of salts in a granitic batholih on the Canadian Shield, southeastern Manitoba, *Appl. Geochem.*, *19*, 519–560.

Haggerty, R., S. M. Wondzell, and M. A. Johnson (2002), Power-law residence time distribution in the hyporheic zone of a 2nd-order mountain stream, *Geophys. Res. Lett.*, *29*(13), 1640, doi:10.1029/2002GL014743.

Harvey, J. W., and K. E. Bencala (1993), The effect of streambed topography of surface-subsurface water exchange in mountain catchments, *Water Resour. Res.*, *29*, 89–98.

Kirchner, J. W., X. Feng, and N. Collin (2000), Fractal stream chemistry and its implications for contaminant transport in catchments, *Nature*, *400*, 524–527.

O'Loughlin, O. O. (1986), Prediction of surface saturation zones in natural catchments by topographic analysis, *Water Resour. Res.*, *22*, 794–804.

Packman, A. I., and K. E. Bencala (2000), Modeling methods in the study of surface-subsurface hydrologic interactions, in *Streams and Ground Waters*, edited by J. B. Jones and P. J. Mulholland, pp. 45–80, Elsevier, New York.

Shen, H. W., H. M. Fehlman, and C. Mendoza (1990), Bed form resistance in open channel flows, *J. Hydrol. Eng.*, *116*, 799–815.

Thibodeaux, L. J., and J. D. Boyle (1987), Bedform-generated convective-transport in bottom sediments, *Nature*, *325*, 341–343.

Tóth, J. (1962), A theory of groundwater motion in small drainage basins in central Alberta, Canada, *J. Geophys. Res.*, *67*, 4375–4387.

Tóth, J., and G. Sheng (1996), Enhancing safety of nuclear waste disposal by exploiting regional groundwater flow: The recharge area concept, *Hydrogeol. J.*, *4*, 4–25.

Wörman, A., A. I. Packman, H. Johansson, and K. Jonsson (2002), Effect of flow-induced exchange in hyporheic zones on longitudinal transport of solutes in streams and rivers, *Water Resour. Res.*, *38*(1), 1001, doi:10.1029/2001WR000769.

Zijl, W. (1999), Scale aspects of groundwater flow and transport system, *Hydrolgeol. J.*, *7*, 139–150.

J. W. Harvey, Water Resources Discipline, U.S. Geological Survey, 430 National Center, Reston, VA 20192, USA.

L. Marklund and A. Wörman, Department of Biometry and Engineering, Swedish University of Agricultural Sciences, SE-75007 Uppsala, Sweden. (anders.worman@bt.slu.se)

A. I. Packman and S. H. Stone, Department of Department of Civil and Environmental Engineering, Northwestern University, Evanston, IL 60208–3109, USA.